

1 Identification and characterization of specific motifs in 2 effector proteins of plant parasites using MOnSTER.

3 Giulia Calia^{1,2} ¶, Paola Porracciolo^{3,4} ¶, Djampa Kozłowski^{3,4}, Hannes Schuler^{1,5}, Alessandro
4 Cestaro^{2,6}, Etienne G.J. Danchin^{4&} and Silvia Bottini^{3&*}

5 ¹ Free University of Bolzano, Faculty of Agricultural Environmental and Food Science, Bolzano, Italy

6 ² Fondazione Edmund Mach, Research and Innovation Centre, San Michele all'Adige, Italy

7 ³ Université Côte d'Azur, Center of Modeling, Simulation and Interactions, Nice, France

8 ⁴ INRAE, Université Côte d'Azur, CNRS, Institut Sophia Agrobiotech, Sophia-Antipolis, France

9 ⁵ Free University of Bolzano, Competence Centre for Plant Health, Bolzano, Italy

10 ⁶ Institute of Biomembranes, Bioenergetics and Molecular Biotechnologies (IBIOM), National Research Council
11 (CNR), Bari, Italy

12 ¶ contributed as co-first author

13 # contributed as co-last author

14 *Corresponding Author: silvia.bottini@univ-cotedazur.fr

15
16
17 **Short title: MOnSTER allows identification of motifs in effectors of plant**
18 **parasites**

19
20
21 ***To whom correspondence should be addressed:***

22 Silvia Bottini, PhD

23 Hopital l'Archet 3

24 151 route de Saint Antoine de Ginestiere,

25 06200, Nice, France

26 +33(6)30566999

27 silvia.bottini@univ-cotedazur.fr

28 **Abstract**

29 Plant pathogens cause billions of dollars of crop loss every year and are a major threat to global food
30 security. Identifying and characterizing pathogens effectors is crucial towards their improved control.
31 Because of their poor sequence conservation, effector identification in protein sequences predicted from
32 genomes is challenging and current methods generate too many candidates without indication for
33 prioritizing further experimental studies. In most phyla, effectors contain specific sequence motifs which
34 influence their localization and targets in the plant. Although bacterial, fungal and oomycetes effectors
35 have been studied extensively and conserved characteristic motifs have been identified, research on
36 plant-parasitic nematode effectors (PPN) identified some enriched degenerate motifs in only one
37 species so far. The different lifestyles of PPNs might reflect effectors with different functions according
38 to the nematode's specific needs, thus presenting a high variety of characteristic motifs.
39 To circumvent these limitations, we have developed MOnSTER a novel tool that identifies clusters of
40 motifs of protein sequences (CLUMP) and associates a score to each CLUMP. This score encompasses
41 the physicochemical properties of AAs and the motif occurrences. We built up our method to identify
42 discriminant CLUMPs in effector proteins of plant-pathogenic oomycetes. We showed the reliability of
43 MOnSTER by identifying five CLUMPs that correspond to the known motifs: RxLR, -dEER and
44 LxLFLAK-HVLVxxP. Consequently, we applied MOnSTER on PPN effector proteins and identified
45 peculiar motifs in their sequences. We identified six CLUMPs in about 60% of the known nematode
46 effectors. Furthermore, we found that specific co-occurrences of at least two CLUMPs are present in
47 PPN effector sequences bearing protein domains important for invasion and pathogenicity.
48 The potentiality of this tool goes behind the effector proteins and can be used to easily cluster motifs
49 and calculate the CLUMPs score on any set of protein sequences.

50

51 **Keywords**

52 Motif clustering – motif scoring – effectors – plant-parasite interaction – *oomycetes* - *nematodes*
53

54 **Authors summary**

55 Population growth, environmental degradation and climate change are already bringing harm
56 to human communities and the natural world that needs to be addressed rapidly. Ensuring
57 food security for a population that will exceed 9 billion people by 2050 while preserving the
58 environment and biodiversity is a major challenge. Agricultural pathogens, to cause the
59 infection, secrete effector proteins that promote colonization of the host plant. Identifying and
60 characterizing pathogens' effectors is crucial towards understanding how they manipulate the
61 plant and better combat them. Because of their poor sequence conservation, effector
62 identification in protein sequences predicted from genomes is challenging and current methods
63 generate too many candidates without indication for prioritizing further experimental studies.
64 To address these challenges, we have developed a novel tool called MOnSTER, that identifies
65 and score clusters of motifs of protein sequences (CLUMPs). MOnSTER is an easy to use tool
66 that can be included in any pipeline needing motif calling and will be of great use to accelerate
67 both computational and experimental studies relating to protein motif discovery. Altogether our
68 findings provide improvements in the understanding of the mechanisms set up by the
69 pathogens to infect the plant and can elucidate important signatures to block the development
70 of plant-pathogen interactions and allow to engineer of durable disease resistance.

71 Introduction

72 Plant pathogens are a major threat to global food security. To cause the infection, pathogenic organisms
73 secrete effector proteins that promote colonization of the host plant by overcoming the physical barriers
74 of plant cell-walls, suppressing or evading immune perception, and deriving nutrients from host tissues
75 [1]. Therefore, identifying and characterizing pathogens effectors is crucial towards understanding how
76 they manipulate the plant and better combat them. Effector proteins are often specific to pathogens and
77 essential for causing plant pathology, constituting targets of choice for the development of cleaner and
78 more specific control methods [2]–[4]. Because of their poor sequence conservation, effector
79 identification among the set of predicted proteins from the genome (proteome) is challenging and current
80 methods generate too many candidates without further indication for prioritizing experimental studies.
81 Classically, effector proteins are indirectly identified among the predicted secretome based on the
82 presence of a signal peptide for secretion and a lack of transmembrane region [5], [6]. However, these
83 criteria alone suffer from two main limitations. On one side, the secretome comprises many proteins that
84 are not effectors, on the other side some known effectors do not possess signal peptides for secretion.
85 In most phyla, effectors contain specific sequence motifs which target host proteins with distinct roles in
86 the infection process and control virulence [7]. The best-studied example is effectors secreted via the
87 type III secretion system (T3SS) class of Gram-negative bacterial pathogens which are characterized
88 by a specific motif/domain conferring a repertoire of molecular determinants with important roles during
89 infection [8], [9]. However, these features are not conserved in other bacteria. Indeed, gram-positive
90 pathogens and certain phloem- and xylem-colonizers, such as *Candidatus liberibacter* and *Xylella spp.*,
91 do not encode the T3SS. In these bacteria, effector delivery is dependent on the presence of the N-
92 terminal signal peptide, which is required for protein secretion [10]. In fungi, two motifs have been
93 identified in effectors, namely the cysteine-rich motifs and the MAX motif [11]. Another well-
94 characterized example are the effectors of the oomycetes pathogens. Oomycetes are eukaryotic
95 filamentous and heterotrophic microorganisms among which, more than 60% of them parasitize plants
96 [12]. Well-known plant pathogens in oomycetes include late blight of potato, sudden oak death, root rot
97 agents (*Phytophthora* species), and downy mildew *Peronospora* and *Bremia* species [13], [14]. These
98 pathogens code for two notable classes of effector proteins RxLR and Crinkler (CRN), that can be
99 predicted by the occurrence of the related motifs, RxLR, -dEER and LxLFLAK-HVLVxxP in the N-
100 terminal region downstream the signal peptide [15]–[17].

101 Although bacterial, fungal and oomycetes effectors have been studied extensively and characteristics
102 motifs have been identified [18], [19], research on Plant-Parasitic Nematode effectors (PPN) did not
103 identify any consensus motif, conserved across multiple species. The most economically important
104 PPNs are the sedentary Root-Knot Nematodes (RKNs) and cyst nematodes [20]. These sedentary
105 parasites induce the formation of a feeding structure that serves as a constant food source for the
106 nematode. Other PPN are migratory and a whole spectrum of variations exists between endo and ecto
107 parasites, with semi-endoparasites an intermediate between the two extremes [21]. The different
108 lifestyles of PPNs are expected to be reflected in their secretions, which presumably contain effectors
109 with different functions according to the nematode's specific needs, thus presenting a high variety of
110 characteristic motifs complicating their identification.

111 A first step toward the identification of motifs characteristics of RKN effectors was performed by Vens et
112 al. [22]. The authors developed a bioinformatic tool, called MERCI, to identify motifs with high
113 occurrences in a positive dataset (known effector sequences) and absent in the negative one (non-
114 effector sequences). MERCI uses a graph-based approach incorporating physicochemical features of
115 the amino acids composing protein sequences. By analyzing the known effector sequences of the RKN
116 species *Meloidogyne incognita*, one of the most important known crop pathogens among all [23], they
117 identified 4 motifs. However, at the time of their publication, very few genomes for RKN species were
118 available, and the study was therefore conducted on one single RKN species. Furthermore, the genome
119 used at that time was later shown to be partially incomplete [24]. These limitations prevent the
120 generalization of the previous findings. Therefore, there is an urgent need for a novel study of the
121 properties of PPN effector sequences and motif research.

122 By taking advantages of the multitude of proteomes available nowadays for several PPN, we developed
123 a comprehensive motif mining analysis to identify characteristic motifs of effector sequences of these
124 species. Sequence motifs are usually of constant short size and are often repeated and conserved.
125 Typically, motifs conform to a particular sequence pattern, where certain positions can be constrained
126 to a specific amino acid, whereas others are not [25]. This confers a high degeneration of the motifs
127 yielding to a huge list of non-redundant motif sequences and consequently some motifs that are not
128 characteristics of effector sequences only [26]. Furthermore, different amino acids (AAs) can have
129 similar physicochemical properties, thus different motif sequences can share similar properties.
130 However, most available motif discovery tools do not take these properties into consideration. To
131 circumvent these limitations, we have developed MOnSTER a novel tool that identifies clusters of motifs
132 of protein sequences (CLUMP) and associates a score to each CLUMP. This score encompasses the
133 physicochemical properties of AAs and the motif occurrences.

134
135 We built-up our method to identify discriminant CLUMPs in 1743 effector proteins of plant-pathogenic
136 oomycetes. We showed the reliability of MOnSTER by identifying 5 CLUMPs that correspond to the
137 known motifs: RxLR, -dEER and LxLFLAK-HVLVxxP. After this proof of concept, we applied MOnSTER
138 on PPN effector proteins and identified peculiar motifs in their sequences at an unprecedented level.
139 We selected a set of 4395 protein sequences from 13 PPN species belonging to the genera
140 *Meloidogyne*, *Globodera*, *Heterodera*, *Radopholus* and *Bursaphelenchus*. We identified 6 CLUMPs
141 present in 60% of the known effectors (positive dataset). Of note these CLUMPs were found in only 5%
142 of the sequences of the negative datasets, thus highlighting the enrichment of the identified motifs in
143 effector sequences. Furthermore, we found a specific co-occurrences of at least two CLUMPs in PPN
144 effector sequences bearing protein domains important for invasion and pathogenicity.

145
146 The potentiality of this tool goes behind the effector proteins and can be used to easily cluster motifs
147 and calculate the CLUMPs score on any set of protein sequences. Furthermore, we also provide a new
148 scoring system capable of measuring the physicochemical properties of motifs grouped in CLUMPs and
149 a motif alignment algorithm to better explore chemical-physical properties within the CLUMPs.
150 MOnSTER is freely available at https://github.com/paolaporracciolo/MOnSTER_PROMOCA.git.

151 **Materials and methods**

152 **Datasets**

153

154 **Oomycetes**

155 We used proteins from five oomycetes species to create the input datasets for MOnSTER, namely
156 *Phytophthora infestans*, *Phytophthora sojae*, *Phytophthora ramorum*, *Hyaloperonospora arabidopsidis*
157 and *Bremia lactucae*.

158

159 **Positive dataset**

160 The positive dataset consists of 1743 effector proteins belonging to the aforementioned oomycetes
161 obtained from a concatenation of proteins selected from PHI-base database (v4.14) [26], Uniprot
162 (release 2023_02)[28], and the work of Haas et al., (2009) [28], in which they have manually curated
163 the annotations of the proteins. Since the proteins come from different sources, we used CD-HIT (v4.8.1)
164 [29] with the parameters in **Supplementary information**, to filter out identical protein sequences. A total
165 of 1283 proteins are annotated as RxLR effectors, 377 as Crinkler effectors and the last 83 sequences
166 are proteins with no previously identified motif and known to be involved in the host-pathogen interaction.

167

168 **Negative dataset**

169 Proteins in the negative dataset derive all from Uniprot (release 2023_02) and from the oomycetes
170 species cited before filtered from proteins included in the positive dataset and for evident effector-related
171 annotations. Due to the large amount of non-effector proteins remaining from the filtering we firstly used
172 'cd-hit' to reduce protein sequence redundancy and then, to also reduce the unbalance of the final
173 dataset we refined the selection taking only the representative sequences of the orthogroups found with
174 Orthofinder (v2.5.4) [30]. In total 3009 non effector proteins are included in the negative dataset.

175

176 **Motif Discovery**

177 The last input file consists in a list of motifs identified as enriched in the sequences of the positive dataset
178 compared to the sequences of the negative one. We used MERCI and STREME (v5.5.1) [31], with
179 parameters detailed in **Supplementary information** [32]. We imposed different lengths for motifs
180 prediction to be inclusive but more stringent on the motifs in which we are interested. STREME's output
181 is a list of motifs. Hence, we used the tool FIMO (v5.5.1) [33], with default parameters to extract 246
182 degenerated motifs from the 4524 different motifs.

183 We obtained the following numbers of non-redundant motifs: 19 with MERCI and 246 with STREME.
184 Then, we removed the identical motifs and created a single non-redundant list containing all the motifs
185 in the same format, which resulted in 265 different motifs.

186

187 **Plant Parasitic Nematodes (PPNs)**

188

189 **Positive dataset**

190 The positive dataset contains proteins selected to be likely secreted by PPNS in their plant host and
191 belonging to 13 species (*Meloidogyne incognita*, *Meloidogyne javanica*, *Meloidogyne arenaria*,

192 *Meloidogyne hapla*, *Meloidogyne chitwoodi*, *Meloidogyne graminicola*, *Globodera rostochiensis*,
193 *Globodera pallida*, *Heterodera havenae*, *Heterodera glycines*, *Heterodera schachtii*, *Radopholus similis*,
194 *Bursaphelenchus xylophilus*). We could identify a part of these proteins as Ground-Truth (GT) effectors
195 based on their literature description. More precisely we considered as GT effectors those proteins for
196 which *in-situ* hybridization experiments showed that the corresponding transcript is present in nematode
197 secretory glands (dorsal or sub-ventral), implying that these proteins are likely secreted by the
198 nematodes into the host plant. The literature mining led to the extraction of 163 proteins from NCBI
199 GeneBank thanks to the NCBI 'entrez' API. We also manually extracted 41 sequences from the
200 publications' core text and Supplementary information. In addition, we downloaded 41 sequences from
201 WormBase ParaSite (www.parasite.wormbase.org, vWBPS17-WS282 [34], [35]), and eight sequences
202 from nematode.net [36]. In total we obtained 229 GT effectors. We extended the positive dataset with
203 proteins that are non-redundant homologs of the previous GT effectors in PPN proteomes. We first used
204 cd-hit-2D with parameters in **Supplementary information**, to cluster sequences from PPNs proteomes
205 and GT effectors [37]. We then pooled all the GT effectors from closely related *Meloidogyne* species
206 (e.g., *M. incognita*, *M. javanica* and *M. arenaria*) and scanned each corresponding proteome with this
207 multi-species set of sequences using cd-hit. Since the remaining species are genetically distinct, we
208 then scanned each proteome with the relative set of GT effectors, except for *H. havenae* and *M.*
209 *chitwoodi* for which no proteomes were currently available. We merged the two set of selected effectors
210 and we performed CD-HIT intra- and inter-species to reduce dataset redundancy (parameters in
211 **Supplementary information**), retaining only sequence having more than 1% divergence and aligning
212 on more than 80% of their length (the longest sequence from each cluster was kept). The final positive
213 dataset includes 546 proteins from 13 species.

214 215 **Negative dataset**

216 The negative dataset is composed of 3849 protein sequences that we obtained by selecting genes
217 widely conserved across the nematode tree of life and close outgroup species, including many species
218 that are non-parasites. Specifically, we filtered the results from a previous analysis [38] and only retained
219 genes from orthogroups i) conserved in more than 90% (62/64) of the analyzed species including two
220 tardigrade species (outgroups), and ii) presenting less than 10 genes/species/orthogroups to avoid
221 multigenic families, which would lead to overrepresentation of some proteins. To remove the
222 redundancy, we used the same strategy as for the positive dataset (cdhit2D first and then CD-HIT).

223 224 **Motif Discovery**

225 Using the aforementioned software in the same configuration we obtained the following numbers of non-
226 redundant motifs: 40 with MERCI and 229 with STREME applying FIMO. In total, we obtained 269
227 different motifs.

228
229 All datasets are available at https://github.com/paolaporracciolo/MOnSTER_PROMOCA.git and in
230 **Supplementary tables 1.1-1.2 and 2.1-2.2.**

231
232

233 **MONSTER pipeline**

234

235 The MONSTER (MOTifs of cluSTERs) pipeline is composed of three main steps as described in **Figure**
236 **1** and in the following paragraphs.

237

238 **Feature calculation**

239 The first step of the pipeline concerns the calculation of parameters that describe protein sequences
240 (**Figure 1a**). To allow an easy calculation of the features on any dataset, we used *ProteinAnalysis*
241 class from the *Bio.SeqUtils.ProtParam*, a python sub-package. We selected 13 features based on
242 individual AA properties, belonging to 4 categories:

- 243 • secondary structure propensity ‘helix’ (V, I, Y, F, W, L), ‘turn’ (N, P, G, S), and ‘sheet’ (E, M, A,
244 L)).
- 245 • amino-acids dimensions (‘tiny’ (A, C, G, S, T) and ‘small’ (A, C, F, G, I, L, M, P, V, W, Y)).
- 246 • pH (‘basic’ (H, K, R), ‘acid’ (B, D, E), and ‘charged’ (H, K, R, B, D, E)).
- 247 • physicochemical properties (‘hydropathy-score’, ‘polar’ (D, E, H, K, N, Q, R, S, T), ‘non-polar’
248 (A, C, F, G, I, L, M, P, V, W, Y), ‘aromatic’ (F, H, W, Y), and ‘aliphatic’ (A, I, L, V)).

249 We performed feature calculations on the positive and negative datasets and the list of motifs. At the
250 end of this step, we obtained three tables of features, one for each of the input datasets (positive,
251 negative datasets and the list of motifs).

252

253 **Clustering**

254 This step allowed to cluster motifs based on their properties described by the 13 features. To make the
255 features comparable to each other, we performed data normalization by using the *StandardScaler*
256 method from *sklearn.preprocessing* [39]. This normalization consists of the removal of the mean and
257 the scaling to unit variance.

258 Then, we performed a hierarchical clustering of the motifs using the Euclidian distance. We then divided
259 the resulting tree into clusters of motifs of proteins (CLUMPs) selecting the threshold distance that
260 minimized the Davies-Bouldin score [40].

261 For each CLUMP, we removed the redundant motifs. Briefly, we identified motifs that shared a core
262 sequence (for example: ‘HWT in HWTQ’ and ‘GHWTQ’), and we only retained the cores (for instance:
263 “HWT”) in the CLUMPs.

264

265 **Scoring**

266 The final objective is to identify the CLUMP(s) with the highest discriminative power concerning the
267 positive dataset. Thus, we conceived a new score called the MONSTER score, to rank the CLUMPs by
268 their discriminative power.

269 The MONSTER score is composed of three parts: the CLUMP score and two modified versions of the
270 Jaccard index.

271

272 **CLUMP score**

273 This score considers the AA composition of the motifs belonging to each CLUMP concerning the
274 preferences of the sequences of the positive dataset. The procedure that we implemented to calculate
275 this score is shown in **Figure 1b**.

276

277 a) Feature selection

278 We used the Mann-Whitney test to identify the features whose values were significantly different
279 between the positive and negative datasets. We only retained the statistically significant features, with
280 a p-value < 0.05. Then, we assigned them a score, by calculating $-\text{Log}(\text{p-value})$ of each feature. We will
281 refer to it as the 'feature weight' hereafter.

282

283 b) Average calculation

284 For each of the selected features, we calculated the average value for the positive dataset, the negative
285 dataset, and each CLUMP that we will refer to with this notation: μ_f^+ , μ_f^- and $\mu_f^{CLUMP_c}$, respectively.

286

287 c) CLUMPs sorting

288 We compared the averages of the positive and negative datasets for each feature and sorted CLUMPs
289 accordingly.

290 Thus, if the $\mu_f^+ \geq \mu_f^-$, the CLUMPs averages would be sorted in ascending order.

291 Otherwise ($\mu_f^+ < \mu_f^-$), CLUMPs averages would be sorted in descending order.

292

293 d) CLUMPs voting

294 For each feature, we divided the CLUMPs into two groups accordingly to the following statements:

295 If $\mu_f^+ \geq \mu_f^-$: CLUMPs with $\mu_f^{CLUMP_c} \geq \mu_f^+$ have a vote from 1 to the number of CLUMPs with an increment
296 of 1, otherwise the score is set to 0.

297 If $\mu_f^+ < \mu_f^-$: CLUMPs with $\mu_f^{CLUMP_c} < \mu_f^+$ the vote attributed goes from 1 to the number of CLUMPs,
298 otherwise it is 0.

299

300 e) CLUMPs scoring

301 For each CLUMP, for each feature, we multiplied the 'feature weight' by the CLUMPs vote then we
302 summed all the results using the following formula:

$$CLUMP_{score} = norm\left[\left(\sum vote_f^{CLUMP_c} xP_f\right)\right]$$

303

304 where we normalized the value to have a range between 0 and 1.

305

306 **Modified Jaccard indexes**

307 The two modified Jaccard scores respectively consider: i) the occurrences of the motifs, for each
308 CLUMP, in the positive dataset compared to the negative, and ii) the number of positive sequences
309 containing the motifs in each CLUMP concerning the negatives (**Figure 1c**).

310

311 a) CLUMPs occurrences

312 We calculated the occurrences of the motifs in each CLUMPs in the two datasets (positive and negative).

313

314 b) J's scores

315 The Jaccard index consists in calculating the similarity between two sets. Here we propose two ways to
316 calculate the J index that will be called J1 and J2 hereafter.

317

318 To obtain J_1 , we calculated the number of occurrences of the motifs for each CLUMP in the negative
319 dataset over the number of occurrences of the motifs of the CLUMP in the positive dataset, using the
320 following equation:

$$J_1 = \sum_{CLUMPs} \frac{1}{2}$$

321 Where:

322 Δ_- and Δ_+ the number of occurrences of the motifs of the CLUMP in the negative or
323 in the positive dataset, respectively.

324

325 To obtain J_2 , for each CLUMP, we calculated the number of sequences of the negative dataset that
326 contain at least a motif of the CLUMP, over the number of sequences of the positive dataset that contain
327 at least a motif of the CLUMP, accordingly to the following formula:

$$J_2 = \sum_{CLUMPs} \frac{1}{2}$$

328

329 Where:

330 seq_- is the number of sequences of the negative dataset containing at least a motif of the CLUMP.

331 seq_+ is the number of sequences of the positive dataset containing at least a motif of the CLUMP.

332

333 The $\frac{1}{2}$ factor is applied to have values between 0 and 0.5 for each J to have equal weight in the final
334 score, and $(1 - \text{Jaccard Index})$ is to consider the degree of dissimilarity rather than similarity.

335

336 **MOnSTER score**

337 The final MOnSTER score, for each CLUMP, is the sum of the CLUMP score, and the two J's indexes:

338

$$339 \quad MOnSTERscore = CLUMP_{score} + J_1 + J_2$$

340

341

342 **PRO-MOCA: a novel method to create motif logo of CLUMPs**

343

344 To create motif logos for each CLUMP, we developed a novel method. PRO-MOCA (PROtein-MOTifs
345 Characteristics Aligner) aligns protein motifs based on the characteristics of the amino acids as shown
346 in **Supplementary figure 1**. The first step is to define the alphabets associated with each characteristic
347 that can be used to represent the motifs (**Supplementary figure 1a**). We have defined four alphabets,
348 namely: “chemical”, “hydrophobicity”, “charge”, “secondary structure propensity” (details for each
349 alphabets are included in the **Supplementary information**).

350 These alphabets are easily modifiable and other alphabets can be included. Different CLUMP logos can
351 be obtained depending on the alphabet chosen. Secondly, PRO-MOCA uses the selected alphabet to
352 translate the AA sequences of each motif in a CLUMP in the new alphabet (**Supplementary figure 1b**).
353 The third step is the alignment (**Supplementary figure 1c**). Briefly, PRO-MOCA screens the translated
354 motif sequences of a CLUMP looking for a “summit position” with the highest frequency of the same
355 “letter” of the novel alphabet (further details in supplementary materials). Once this position is identified,
356 all motifs are aligned accordingly (**Supplementary figure 1d**). Since the motifs of a CLUMP can have
357 different lengths, after the alignment, PRO-MOCA calculates the number of gaps to add at the
358 extremities to make all motifs having the same length. Importantly, gaps are not allowed inside the motif
359 sequences. The last step of the method is to re-translate the aligned motifs in the original AA sequences
360 (**Supplementary figure 1e**). The alignment is ready to feed a program to create logos. Here we used
361 the tool Weblogo3 [41].

362

363 **PPNs effector protein domains mining analysis**

364

365 To investigate the relationship between the selected CLUMPs and functional domain in effector proteins
366 we firstly selected proteins from the positive datasets containing at least one occurrence of a selected
367 CLUMP (311 proteins in total). Then we predicted the protein domains with InterProScan (v5.54-87.0)
368 [42] with default parameters. From the results, we extracted the proteins containing the most frequent
369 predicted domains and considered only entries coming from: MobiDB-lite, Coils, CDD, PANTHER, Pfam
370 and ProSitePatterns. Afterwards we also predicted the presence of Signal Peptide (SP) (SignalP4.1
371 [43]) and TransMembrane (TM) domain regions (TMHMM2.0 [44]). We obtained 258 proteins having at
372 least a CLUMP and one of the aforementioned predicted domains, SP or TM.

373 **Results & Discussion**

374

375 **MOnSTER identified five CLUMPs containing known motifs characteristics of** 376 **oomycetes effector protein sequences**

377

378 Characteristic motifs of oomycetes effector proteins are well-known in the literature, such as RxLR, -
379 dEER and LxLFLAK-HVLVxxP [15]. Thus, we reasoned to apply our novel tool, MOnSTER, on
380 oomycetes effectors to test its ability to recover well-characterized motifs. We compiled a set of 4752
381 oomycetes proteins, comprising 1743 effectors and 3009 non effectors, from five oomycetes species.
382 We performed motif discovery on this set of proteins using MERCI and STREME and we identified 265
383 significantly enriched motifs (see methods for further details). Then we fed MOnSTER with these motifs
384 and we obtained 11 CLUMPs (**Supplementary table 3**), employing the Davis-Bouldin score, as a
385 criterion to cut the tree. By selecting CLUMPs having a MOnSTER score greater than the median of the
386 overall scores we identified six CLUMPs (CLUMP7, 4, 10, 6, 2 and 9), the first five best-scoring CLUMPs,
387 accordingly to the MOnSTER score, correspond to the known motifs (**Figure 2**). In **Supplementary**
388 **figure 2** we can also observe that the motifs are respectively grouped in two clades, the two
389 characteristics motifs of CRN-effectors (LxLFLAK and HVLVxxP), form a separate subclade on the right,
390 while the RxLR and -dEER motifs fall into the left clade, resembling the family distinction of effectors to
391 which they belong. More precisely RxLR motifs are divided into 2 different CLUMPs; CLUMP6 containing
392 only RYLR and RFLR motifs, and CLUMP10, containing other RxLR motifs and included in the same
393 sub-clade of the dEER motif (CLUMP2). The last best-scoring CLUMP contains no known motifs,
394 perhaps suggesting a novel putative motif for oomycetes effectors to investigate. Since oomycetes
395 effectors characterization is not in the scope of this article, we did not consider this last CLUMP for
396 further analysis. In support of that, CLUMPs 7, 4, 10, 6 and 2 are present in 1205/1743 effectors (~70%
397 of the sequences in the positive dataset) while in combination with the last significant CLUMP (CLUMP9)
398 only 2 more sequences can be detected.

399 Thus, we investigated the occurrences and co-occurrences of the five selected CLUMPs in oomycetes
400 effectors and non-effectors (**Supplementary figure 3**). For the effectors we deeply analyzed the two
401 distinct families; in total we found that 68% of the RxLR-effectors in the positive dataset contain the
402 motifs in CLUMPs associated with the RxLR motif (CLUMP10, 6 and 2). In particular, CLUMP10 and 6
403 are present alone in 41% of the RxLR-effectors (1238/1743 RxLR-effectors), while 19% of the RxLR-
404 effectors contained the co-occurrence of these CLUMPs with the CLUMPs representing the dEER motif
405 (CLUMP2). This reflects the importance of the RxLR motifs in the effector sequences and the role of the
406 attached dEER [45]. On the other hand, the co-occurrence of CLUMPs specific for LxLFLAK and
407 HVLVxxP (CLUMP7 and 4), in CRN-effector sequences accounts for 67% of the relative sequences in
408 the positive dataset (377/1743). The high co-occurrences rate of CLUMP7 and 4 is strongly in
409 agreement with the presence of LxLFLAK and HVLVxxP motif marking the beginning and the end of
410 the DWL-domain in the Crinkler-effector family [28]. For the negative dataset, instead, only 15% of the
411 sequences show the presence of CLUMP-motifs with a huge decrease in CLUMPs co-occurrences.
412 Overall co-occurrences, indeed, are present in around 30% of positive sequences and in 1% of negative
413 ones.

414 Previous research showed that the motifs characteristics of oomycetes effectors have strong sequence
415 position preferences [46]–[48]. Thus, we plotted the CLUMPs occurrences in the positive versus
416 negative dataset (**Supplementary figure 4**). Indeed, we can observe that the CLUMPs are concentrated
417 at the beginning of the sequence in positive sequences and conversely spread around the sequence of

418 negative dataset proteins. More precisely the 5 most interesting CLUMPs are condensed in the first 40%
419 of the sequence with a higher preference at the very beginning and around 30% of the sequence
420 probably corresponding to the N-terminal of the protein in which the target motifs lie.
421 Altogether these results highlight the ability of MOnSTER to identify CLUMPs containing biologically
422 relevant motifs.

423

424 **MOnSTER allowed to identify six CLUMPs characteristics of nematodes effector** 425 **proteins** 426

427 The application of MOnSTER of the oomycetes effectors served as a proof of concept of our
428 methodology. Thus, we moved to the characterization of nematodes effector sequences for which no
429 characteristic motifs have been identified yet. We collected a set of 4395 proteins, including 546 well-
430 known effectors and 3849 non-effectors, coming from 13 nematode species. By running motif discovery
431 analysis as for the previous dataset, we found 269 motifs enriched in the effectors sequences. By
432 applying MOnSTER with the previous configuration, the 269 input motifs were grouped into 11 CLUMPs.
433 Six best-scoring CLUMPs were selected using the median as the significative threshold
434 (**Supplementary table 4**). Similar to the oomycetes results, we observe two main clades (**Figure 3**):
435 the second and the third best scoring ones (CLUMP2 and 5 respectively) form a single clade while the
436 other significant CLUMPs (CLUMP1, 3, 7 and 10) are distributed in the bigger clade with the non-
437 significant ones. Overall, we found CLUMPs in almost 60% of sequences from the positive dataset
438 compared to 5% of sequences from the negative.

439 Then we investigated the presence of the six CLUMPs in each of the 13 PPN species present in the
440 dataset. **Figure 4** shows the abundance of the six best-scoring CLUMPs in the species accordingly to
441 their phylogeny tree. The first three species are the most represented in the positive dataset.
442 Interestingly very distant species show similar CLUMPs frequencies thus suggesting that they might
443 share common characteristics at the sequence level for accomplishing similar functions. Furthermore,
444 we could identify characteristic CLUMPs also for species represented in the dataset with very few
445 sequences reinforcing the previous observation. Overall, this analysis suggests that CLUMPs might be
446 associated with functional properties of PPN nematodes.

447 Finally, we focused on the positional sequence preferences of CLUMPs in effector sequences
448 (**Supplementary figure 5**). In general, we observe a difference in the position preferences of the best-
449 scoring CLUMPs between positive and negative dataset sequences. The 6 CLUMPs tend to occur more
450 frequently in the middle of the sequences in effectors (positive dataset), with more abundance in central
451 (around 50% of the sequence) and terminal (around 70%), positions. The same CLUMPs are rare in the
452 central position of the non-effector protein sequences (negative dataset). Contrary to the properties of
453 oomycetes effectors, which characteristics CLUMPs occur mainly at the beginning of the sequence,
454 PPN effectors showed a different pattern of occurrences, privileging a central – C terminal occurrence.

455

456 **Co-occurrences of different CLUMPs are associated with functional protein domains.** 457

458 We investigated the co-occurrence patterns of CLUMPs in the PPNs effector sequences (all possible
459 combinations of co-occurrences are reported in **Supplementary figure 6**). Overall, we notice that

460 CLUMPs tend to co-occur more frequently in the sequences of the positive dataset than in the negative
461 one, despite the positive set being smaller than the negative one. 30% of effector sequences show co-
462 occurrences of the 6 selected CLUMPs, while in the non-effectors, co-occurrences, are present in less
463 than 1% of the sequences. As observed for oomycetes, some CLUMPs tend to be present alone, while
464 others tend to co-occur with specific CLUMPs. This suggests that different classes of nematode effectors
465 might exist, similar to the oomycetes effectors. Importantly, there is no relationship between the
466 sequence length and the number of co-occurrences that might suggest a functional role for CLUMPs
467 co-occurrences (**Supplementary figure 7**).

468 To inspect further a putative functional role of CLUMPs in effector sequences, we queried the effectors
469 having at least one CLUMP or a co-occurrence of multiple CLUMPs against several protein domain
470 databases (see Methods, results in **Figure 5** and **Supplementary table 5**). The most recurrent hits are
471 the coil domain, intrinsically disordered domain and the presence of the signal peptide (SP) followed by
472 the pectate lyase domain, glycosyl hydrolase family 5, Stichodactyla toxin (ShK) domain, 14-3-3 family
473 and cysteine-rich domain. Interestingly, we observe the almost exclusive association between CLUMPs
474 and functional domains, mainly when multiple CLUMPs co-occur in effector sequences.

475 The strongest association that we observe is between the co-occurrences of CLUMPs 7 and 10 and the
476 glycosyl hydrolase family 5 domain on one hand and the co-occurrences of CLUMPs 3, 7, 10 and the
477 cysteine-rich domain, on the other hand. Specifically, all 23 effector sequences containing the co-
478 occurrences of CLUMP 7 and 10 bear also the glycosyl hydrolase family 5 domain. By inspecting the
479 position of CLUMPs occurrences within the sequences, we observed that the two CLUMPs are flanking
480 the domain: CLUMP7 is consistently present at the beginning of the sequence and consequently of the
481 domain, while CLUMP10 mostly concentrates at the end of the domain, around 60-80% of the
482 sequences (**Supplementary figure 8**). Examples of these genes in nematodes is poorly characterized
483 and likely resulting from horizontal transfer [49], [50]. Similarly, all 17 sequences presenting the co-
484 occurrence of CLUMPs 3, 7,10 also contain the cysteine-rich domain. Cysteine-rich domain and CAP
485 protein are known to be involved in the virulence of nematodes [51]. They are expressed in both plants
486 and pathogens; in the latter, they are important for their virulence by suppressing the host's immune
487 responses and promoting colonization. Interestingly, these sequences do not contain disordered regions
488 or coil domains, consistently with unique conserved sandwich fold with a large central cavity of these
489 kinds of proteins [52]. 16 out of 19 sequences presenting co-occurrences of CLUMPs 2, 3 have also the
490 14-3-3 family domain, a eukaryotic-specific protein family with a general role in the signal transduction
491 [53]. We also observe only one motif from CLUMP 2 in these sequences (KDKM) and 4 from CLUMP 3
492 (NKDKAC, KMKG, PTHPIR, PTHP). 13 out of 34 sequences bearing only CLUMP 1 also contain the
493 pectate lyase domain. Of note, these sequences do not contain coiled or disordinate regions, and only
494 7 show the presence of the SP. Pectate lyase enzymes in nematodes facilitate penetration in plant-cell
495 walls made of pectin [54]. numerous recent reports showed that these enzymes are produced in
496 specialized nematode gland cells and secreted during the parasitism process. In the case of sedentary
497 endo-parasitic nematodes, this occurs mainly during juvenile migration through the root tissue, when
498 these enzymes play a crucial role in the maceration of the plant tissue facilitating the infection [55].
499 Finally, 8 out of 22 sequences bear the co-occurrences of CLUMPs 2, 5 and the ShK domain. Although

500 the exact biological function of the ShKT domain remains unclear, previous reports have shown that this
501 domain might be associated with immunosuppression [56], [57].

502 Overall, these findings highlight that specific CLUMPs co-occurrences are associated with specific
503 functional domains with roles in invasion and/or infection and might suggest different classes of effectors
504 cross-species.

505

506 **Conclusions**

507 This work is structured around three main aims: (1) the development of a novel method to cluster and
508 score discriminant motifs of protein sequences called MOnSTER, (2) the validation of the MOnSTER
509 results by applying it to identify CLUMPs specific to effector protein sequences of oomycetes (3) the
510 application of MOnSTER to protein sequences from plant-parasitic nematodes with unprecedented
511 discriminant motifs detection.

512 The application of MOnSTER on oomycetes yielded the identification of five CLUMPs corresponding to
513 the well-known effector-related motifs like RxLR-dEER and LxLFLAK-HVLVxxP motifs in oomycetes.

514 This demonstrated that the novel scoring method introduced by MOnSTER is a good parameter with
515 which calculate CLUMP specificity for effector protein sequences. When applied on the nematodes
516 effectors, MOnSTER found six novel CLUMPs, not previously characterized. The main advantage of
517 MOnSTER is that the definition of CLUMPs allowed us to reduce the degeneration of 265 and 269 motifs
518 (oomycetes and nematodes respectively), to 11 CLUMPs. Effectors sequences of both pathogens show
519 some common characteristics. Indeed, selected CLUMPs-motifs are present in about 70% of the input
520 effector proteins for oomycetes and 60% in PPN compared to 15% and 5% in of the non-effector
521 proteins, respectively. Furthermore, around 30% of effector sequences have co-occurring CLUMPs, in
522 contrast with less than 1% of the non-effector sequences, in both applications. The main difference
523 between effector-specific motifs of the two pathogens is the positional preference: the beginning of the
524 sequence for oomycetes and central C-terminal for PPNs. This highlights MOnSTER ability to cluster
525 motifs specifically relevant for effector sequences without privilege any portion of the sequence, like
526 other motif discovery tools.

527 Concerning the novel identified motifs for PPNs effectors, we observed that the pattern of occurrences
528 and co-occurrences of CLUMPs in effector sequences is associated with specific functional domains
529 and might suggest the existence of different classes of effectors. Importantly we did not observe any
530 species-related preferences thus implying the generality of these results.

531 In conclusion, MOnSTER quantifies the motifs and sequence properties in each dataset provided, thus
532 allowing a wide application to other protein classes. Since the MOnSTER score considers the
533 physicochemical properties and occurrences of motifs in CLUMPs concerning the protein sequences
534 provided, it works without the need for a reference dataset. Furthermore, the MOnSTER scores are
535 normalized values, therefore, allowing direct comparison between different studies.

536 Our results highlighted that MOnSTER is a powerful new method to cluster and score discriminant motifs
537 in protein sequences according to their physicochemical properties and pattern of occurrences. It is also
538 a tool that can be easily used on any set of protein sequences and a list of motifs. As such, MOnSTER

539 can be included in any pipeline needing motif calling and will be of great use to accelerate both
540 computational and experimental studies relating to protein motif discovery.
541
542

543 **Data availability**

544 The source code and related data are available at:
545 https://github.com/paolaporracciolo/MOnSTER_PROMOCA.git

546 **Funding**

547 This work was supported by the French government, through the UCA JEDI Investments in the Future
548 project managed by the National Research Agency (ANR) under reference number ANR-15-IDEX-01.

549 **Competing Interests**

550 The authors declare that they have no competing interests.
551

552 **References**

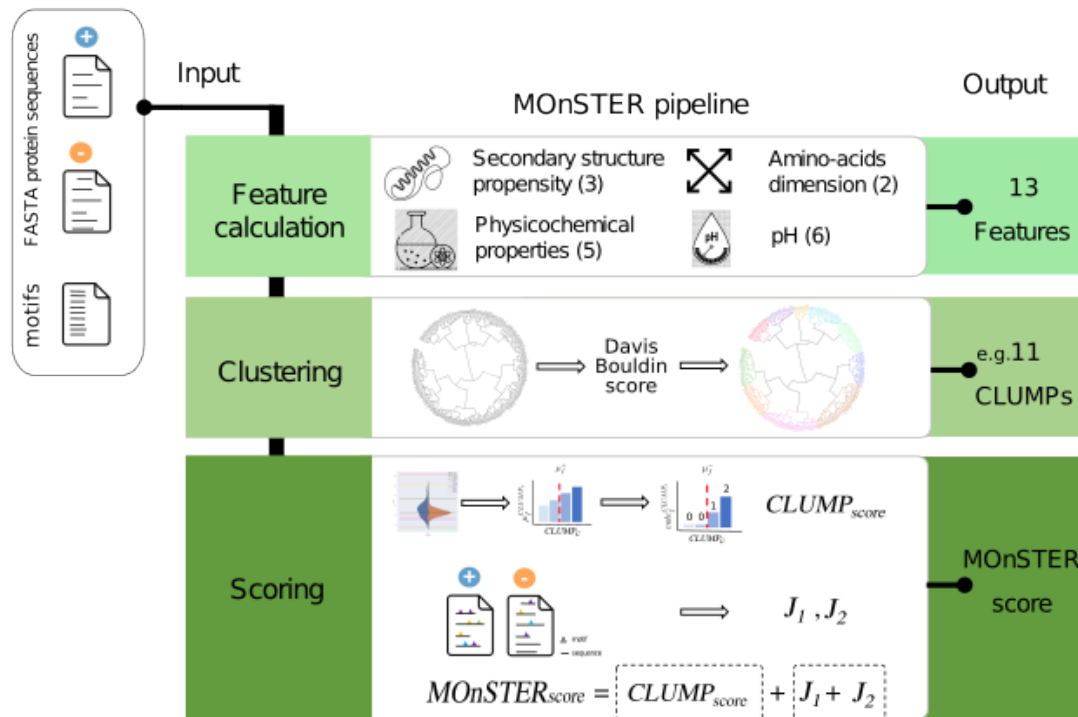
- 553
554 [1] T. Y. Toruño, I. Stergiopoulos, and G. Coaker, "Plant-Pathogen Effectors: Cellular Probes
555 Interfering with Plant Defenses in Spatial and Temporal Manners," *Annu. Rev. Phytopathol.*, vol.
556 54, pp. 419–441, Aug. 2016, doi: 10.1146/annurev-phyto-080615-100204.
557 [2] A. Haegeman, S. Mantelin, J. T. Jones, and G. Gheysen, "Functional roles of effectors of plant-
558 parasitic nematodes," *Gene*, vol. 492, no. 1, pp. 19–31, Jan. 2012, doi:
559 10.1016/j.gene.2011.10.040.
560 [3] C. Selin, T. R. de Kievit, M. F. Belmonte, and W. G. D. Fernando, "Elucidating the Role of Effectors
561 in Plant-Fungal Interactions: Progress and Challenges," *Front. Microbiol.*, vol. 7, 2016, [Online].
562 Available: <https://www.frontiersin.org/articles/10.3389/fmicb.2016.00600>
563 [4] D. M. Bird, J. T. Jones, C. H. Opperman, T. Kikuchi, and E. G. J. Danchin, "Signatures of
564 adaptation to plant parasitism in nematode genomes," *Parasitology*, vol. 142 Suppl 1, no. Suppl
565 1, pp. S71-84, Feb. 2015, doi: 10.1017/S0031182013002163.
566 [5] J. Sperschneider *et al.*, "Evaluation of Secretion Prediction Highlights Differing Approaches
567 Needed for Oomycete and Fungal Effectors", *Frontiers in Plant Science*, vol. 6, 2015,
568 doi:10.3389/fpls.2015.01168.
569 [6] H. Sonah and R.K. Deshmukh, "Computational Prediction of Effector Proteins in Fungi:
570 Opportunities and Challenges", *Front Plant Sci.*, vol. 12, pp. 7:126, Feb. 2016,
571 doi:10.3389/fpls.2016.00126.
572 [7] L. Liu *et al.*, "Arms race: diverse effector proteins with conserved motifs," *Plant Signal. Behav.*, vol.
573 14, no. 2, p. 1557008, Jan. 2019, doi: 10.1080/15592324.2018.1557008.
574 [8] P. Dean, "Functional domains and motifs of bacterial type III effector proteins and their roles in
575 infection," *FEMS Microbiol. Rev.*, vol. 35, no. 6, pp. 1100–1125, Nov. 2011, doi: 10.1111/j.1574-
576 6976.2011.00271.x.
577 [9] E. R. Green and J. Meccas, "Bacterial Secretion Systems: An Overview," *Microbiol. Spectr.*, vol.
578 4, no. 1, Feb. 2016, doi: 10.1128/microbiolspec.VMBF-0012-2015.
579 [10] P. Natale, T. Brüser, and A. J. M. Driessen, "Sec- and Tat-mediated protein secretion across the
580 bacterial cytoplasmic membrane—Distinct translocases and mechanisms," *Biochim. Biophys.*
581 *Acta BBA - Biomembr.*, vol. 1778, no. 9, pp. 1735–1756, Sep. 2008, doi:
582 10.1016/j.bbamem.2007.07.015.
583 [11] J. Sperschneider, P. N. Dodds, D. M. Gardiner, J. M. Manners, K. B. Singh, and J. M. Taylor,
584 "Advances and Challenges in Computational Prediction of Effectors from Plant Pathogenic Fungi,"
585 *PLOS Pathog.*, vol. 11, no. 5, p. e1004806, May 2015, doi: 10.1371/journal.ppat.1004806.
586 [12] G. W. Beakes, S. L. Glockling, and S. Sekimoto, "The evolutionary phylogeny of the oomycete
587 'fungi,'" *Protoplasm*, vol. 249, no. 1, pp. 3–19, Jan. 2012, doi: 10.1007/s00709-011-0269-2.

- 588 [13] M. Thines and S. Kamoun, "Oomycete-plant coevolution: recent advances and future prospects,"
589 *Curr. Opin. Plant Biol.*, vol. 13, no. 4, pp. 427–433, Aug. 2010, doi: 10.1016/j.pbi.2010.04.001.
- 590 [14] K. J. Wood *et al.*, "Effector prediction and characterization in the oomycete pathogen *Bremia*
591 *lactucae* reveal host-recognized WY domain proteins that lack the canonical RXLR motif," *PLOS*
592 *Pathog.*, vol. 16, no. 10, p. e1009012, Oct. 2020, doi: 10.1371/journal.ppat.1009012.
- 593 [15] M. Franceschetti, A. Maqbool, M. J. Jiménez-Dalmaroni, H. G. Pennington, S. Kamoun, and M. J.
594 Banfield, "Effectors of Filamentous Plant Pathogens: Commonalities amid Diversity," *Microbiol.*
595 *Mol. Biol. Rev.*, vol. 81, no. 2, pp. e00066-16, Mar. 2017, doi: 10.1128/MMBR.00066-16.
- 596 [16] R. H. Y. Jiang, S. Tripathy, F. Govers, and B. M. Tyler, "RXLR effector reservoir in two
597 *Phytophthora* species is dominated by a single rapidly evolving superfamily with more than 700
598 members," *Proc. Natl. Acad. Sci. U. S. A.*, vol. 105, no. 12, pp. 4874–4879, Mar. 2008, doi:
599 10.1073/pnas.0709303105.
- 600 [17] T. A. Torto *et al.*, "EST mining and functional expression assays identify extracellular effector
601 proteins from the plant pathogen *Phytophthora*," *Genome Res.*, vol. 13, no. 7, pp. 1675–1685, Jul.
602 2003, doi: 10.1101/gr.910003.
- 603 [18] L. Pritchard and P. Birch, "A systems biology perspective on plant–microbe interactions:
604 Biochemical and structural targets of pathogen effectors," *Plant Sci.*, vol. 180, no. 4, pp. 584–603,
605 Apr. 2011, doi: 10.1016/j.plantsci.2010.12.008.
- 606 [19] A. H. Lovelace, S. Dorhmi, M. T. Hulin, Y. Li, J. W. Mansfield, and W. Ma, "Effector Identification
607 in Plant Pathogens," *Phytopathology*, vol. 113, no. 4, pp. 637–650, Apr. 2023, doi:
608 10.1094/PHYTO-09-22-0337-KD.
- 609 [20] J. T. Jones *et al.*, "Top 10 plant-parasitic nematodes in molecular plant pathology," *Mol. Plant*
610 *Pathol.*, vol. 14, no. 9, pp. 946–961, Dec. 2013, doi: 10.1111/mpp.12057.
- 611 [21] M. Holterman *et al.*, "Disparate gain and loss of parasitic abilities among nematode
612 lineages," *PloS One*, vol. 12, no. 9, p. e0185445, 2017, doi: 10.1371/journal.pone.0185445.
- 613 [22] C. Vens, M.-N. Rosso, and E. G. J. Danchin, "Identifying discriminative classification-based motifs
614 in biological sequences," *Bioinformatics*, vol. 27, no. 9, pp. 1231–1238, May 2011, doi:
615 10.1093/bioinformatics/btr110.
- 616 [23] R. Blanc-Mathieu *et al.*, "Hybridization and polyploidy enable genomic plasticity without sex in
617 the most devastating plant-parasitic nematodes," *PLOS Genet.*, vol. 13, no. 6, p. e1006777, Jun.
618 2017, doi: 10.1371/journal.pgen.1006777.
- 619 [24] P. Abad *et al.*, "Genome sequence of the metazoan plant-parasitic nematode *Meloidogyne*
620 *incognita*," *Nat. Biotechnol.*, vol. 26, no. 8, pp. 909–915, Aug. 2008, doi: 10.1038/nbt.1482.
- 621 [25] N. E. Davey, M. S. Cyert, and A. M. Moses, "Short linear motifs – ex nihilo evolution of protein
622 regulation," *Cell Commun. Signal.*, vol. 13, no. 1, p. 43, Dec. 2015, doi: 10.1186/s12964-015-0120-
623 z.
- 624 [25] E. D. O. Roberson, "Motif scraper: a cross-platform, open-source tool for identifying degenerate
625 nucleotide motif matches in FASTA files," *Bioinformatics*, vol. 34, no. 22, pp. 3926–3928, Nov.
626 2018, doi: 10.1093/bioinformatics/bty437.
- 627 [26] M. Urban, R. Pant, A. Raghunath, A. G. Irvine, H. Pedro, and K. E. Hammond-Kosack, "The
628 Pathogen-Host Interactions database (PHI-base): additions and future developments," *Nucleic*
629 *Acids Res.*, vol. 43, no. Database issue, pp. D645-655, Jan. 2015, doi: 10.1093/nar/gku1165.
- 630 [27] The UniProt Consortium, "UniProt: the Universal Protein Knowledgebase in 2023," *Nucleic Acids*
631 *Res.*, vol. 51, no. D1, pp. D523–D531, Jan. 2023, doi: 10.1093/nar/gkac1052.
- 632 [28] B. J. Haas *et al.*, "Genome sequence and analysis of the Irish potato famine pathogen
633 *Phytophthora infestans*," *Nature*, vol. 461, no. 7262, Art. no. 7262, Sep. 2009, doi:
634 10.1038/nature08358.
- 635 [29] L. Fu, B. Niu, Z. Zhu, S. Wu, and W. Li, "CD-HIT: accelerated for clustering the next-generation
636 sequencing data," *Bioinformatics*, vol. 28, no. 23, pp. 3150–3152, Dec. 2012, doi:
637 10.1093/bioinformatics/bts565.
- 638 [30] D. M. Emms and S. Kelly, "OrthoFinder: phylogenetic orthology inference for comparative
639 genomics," *Genome Biol.*, vol. 20, no. 1, p. 238, Nov. 2019, doi: 10.1186/s13059-019-1832-y.
- 640 [31] T. L. Bailey, "STREME: accurate and versatile sequence motif discovery," *Bioinformatics*, vol. 37,
641 no. 18, pp. 2834–2840, Sep. 2021, doi: 10.1093/bioinformatics/btab203.
- 642 [32] C. E. Grant, T. L. Bailey, and W. S. Noble, "FIMO: scanning for occurrences of a given motif,"
643 *Bioinformatics*, vol. 27, no. 7, pp. 1017–1018, Apr. 2011, doi: 10.1093/bioinformatics/btr064.
- 644 [33] K. L. Howe *et al.*, "WormBase 2016: expanding to enable helminth genomic research," *Nucleic*
645 *Acids Res.*, vol. 44, no. D1, pp. D774–D780, Jan. 2016, doi: 10.1093/nar/gkv1217.

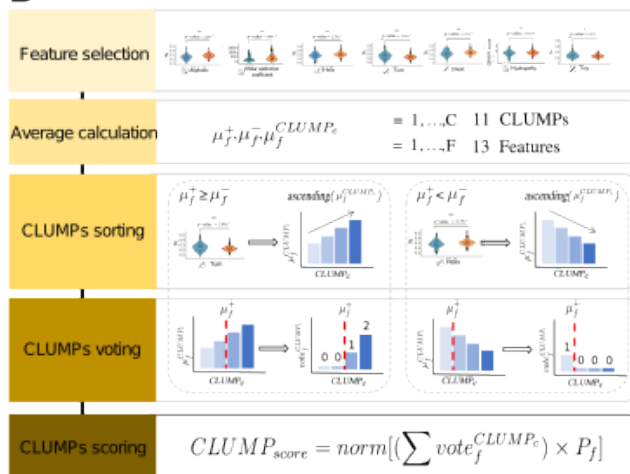
- 646 [34] K. L. Howe, B. J. Bolt, M. Shafie, P. Kersey, and M. Berriman, "WormBase ParaSite –
647 a comprehensive resource for helminth genomics," *Mol. Biochem. Parasitol.*, vol. 215, pp. 2–10,
648 Jul. 2017, doi: 10.1016/j.molbiopara.2016.11.005.
- 649 [35] J. Martin *et al.*, "Helminth.net: expansions to Nematode.net and an introduction to Trematode.net,"
650 *Nucleic Acids Res.*, vol. 43, no. D1, pp. D698–D706, Jan. 2015, doi: 10.1093/nar/gku1128.
- 651 [36] W. Li and A. Godzik, "Cd-hit: a fast program for clustering and comparing large sets of protein or
652 nucleotide sequences," *Bioinformatics*, vol. 22, no. 13, pp. 1658–1659, Jul. 2006, doi:
653 10.1093/bioinformatics/btl158.
- 654 [37] P. Grynberg *et al.*, "Comparative Genomics Reveals Novel Target Genes towards Specific Control
655 of Plant-Parasitic Nematodes," *Genes*, vol. 11, no. 11, p. 1347, Nov. 2020, doi:
656 10.3390/genes11111347.
- 657 [38] R. Blanc-Mathieu *et al.*, "Hybridization and polyploidy enable genomic plasticity without sex in the
658 most devastating plant-parasitic nematodes," *PLOS Genet.*, vol. 13, no. 6, p. e1006777, Jun.
659 2017, doi: 10.1371/journal.pgen.1006777.
- 660 [39] F. Pedregosa *et al.*, "Scikit-learn: Machine Learning in Python," *Mach. Learn. PYTHON*, p. 6.
- 661 [40] D. L. Davies and D. W. Bouldin, "A Cluster Separation Measure," *IEEE Trans. Pattern Anal. Mach.*
662 *Intell.*, vol. PAMI-1, no. 2, pp. 224–227, Apr. 1979, doi: 10.1109/TPAMI.1979.4766909.
- 663 [41] G. E. Crooks, G. Hon, J.-M. Chandonia, and S. E. Brenner, "WebLogo: A Sequence Logo
664 Generator," p. 3.
- 665 [42] P. Jones *et al.*, "InterProScan 5: genome-scale protein function classification," *Bioinformatics*, vol.
666 30, no. 9, pp. 1236–1240, May 2014, doi: 10.1093/bioinformatics/btu031.
- 667 [43] H. Nielsen, "Predicting Secretory Proteins with SignalP," in *Protein Function Prediction: Methods
668 and Protocols*, D. Kihara, Ed., in Methods in Molecular Biology. New York, NY: Springer, 2017,
669 pp. 59–73. doi: 10.1007/978-1-4939-7015-5_6.
- 670 [44] A. Krogh, B. Larsson, G. von Heijne, and E. L. Sonnhammer, "Predicting transmembrane protein
671 topology with a hidden Markov model: application to complete genomes," *J. Mol. Biol.*, vol. 305,
672 no. 3, pp. 567–580, Jan. 2001, doi: 10.1006/jmbi.2000.4315.
- 673 [45] L. S. Boutemy *et al.*, "Structures of Phytophthora RXLR effector proteins: a conserved but
674 adaptable fold underpins functional diversity," *J. Biol. Chem.*, vol. 286, no. 41, pp. 35834–35842,
675 Oct. 2011, doi: 10.1074/jbc.M111.262303.
- 676 [46] S. Schornack *et al.*, "Ancient class of translocated oomycete effectors targets the host nucleus,"
677 *Proc. Natl. Acad. Sci. U. S. A.*, vol. 107, no. 40, pp. 17421–17426, Oct. 2010, doi:
678 10.1073/pnas.1008491107.
- 679 [47] A. P. Rehmany *et al.*, "Differential recognition of highly divergent downy mildew avirulence gene
680 alleles by RPP1 resistance genes from two Arabidopsis lines," *Plant Cell*, vol. 17, no. 6, pp. 1839–
681 1850, Jun. 2005, doi: 10.1105/tpc.105.031807.
- 682 [48] T. M. M. M. Amaro, G. J. A. Thilliez, G. B. Motion, and E. Huitema, "A Perspective on CRN Proteins
683 in the Genomics Age: Evolution, Classification, Delivery and Function Revisited," *Front. Plant Sci.*,
684 vol. 8, 2017, Accessed: Jun. 01, 2023. [Online]. Available:
685 <https://www.frontiersin.org/articles/10.3389/fpls.2017.00099>
- 686 [49] E. G. J. Danchin *et al.*, "Multiple lateral gene transfers and duplications have promoted plant
687 parasitism ability in nematodes," *Proc. Natl. Acad. Sci. U. S. A.*, vol. 107, no. 41, pp. 17651–17656,
688 Oct. 2010, doi: 10.1073/pnas.1008486107.
- 689 [50] H. Aspeborg, P. M. Coutinho, Y. Wang, H. Brumer, and B. Henrissat, "Evolution, substrate
690 specificity and subfamily classification of glycoside hydrolase family 5 (GH5)," *BMC Evol. Biol.*,
691 vol. 12, no. 1, p. 186, Sep. 2012, doi: 10.1186/1471-2148-12-186.
- 692 [51] Z. Han, D. Xiong, R. Schneiter, and C. Tian, "The function of plant PR1 and other members of the
693 CAP protein superfamily in plant–pathogen interactions," *Mol. Plant Pathol.*, vol. 24, no. 6, pp.
694 651–668, 2023, doi: 10.1111/mpp.13320.
- 695 [52] G. M. Gibbs, K. Roelants, and M. K. O'Bryan, "The CAP superfamily: cysteine-rich secretory
696 proteins, antigen 5, and pathogenesis-related 1 proteins—roles in reproduction, cancer, and
697 immune defense," *Endocr. Rev.*, vol. 29, no. 7, pp. 865–897, Dec. 2008, doi: 10.1210/er.2008-
698 0032.
- 699 [53] R. Lozano-Durán and S. Robatzek, "14-3-3 Proteins in Plant-Pathogen Interactions," *Mol. Plant-
700 Microbe Interactions*®, vol. 28, no. 5, pp. 511–518, May 2015, doi: 10.1094/MPMI-10-14-0322-
701 CR.
- 702 [54] K. Wieczorek *et al.*, "A Distinct Role of Pectate Lyases in the Formation of Feeding Structures
703 Induced by Cyst and Root-Knot Nematodes," *Mol. Plant-Microbe Interactions*®, vol. 27, no. 9, pp.
704 901–912, Sep. 2014, doi: 10.1094/MPMI-01-14-0005-R.

- 705 [55] T. Hwezi and T. J. Baum, "Manipulation of plant cells by cyst and root-knot nematode effectors,"
706 *Mol. Plant-Microbe Interact. MPMI*, vol. 26, no. 1, pp. 9–16, Jan. 2013, doi: 10.1094/MPMI-05-12-
707 0106-FI.
- 708 [56] H. Song *et al.*, "The *Meloidogyne javanica* effector Mj2G02 interferes with jasmonic acid signalling
709 to suppress cell death and promote parasitism in *Arabidopsis*," *Mol. Plant Pathol.*, vol. 22, no. 10,
710 pp. 1288–1301, Oct. 2021, doi: 10.1111/mpp.13111.
- 711 [57] J. Niu *et al.*, "Msp40 effector of root-knot nematode manipulates plant immunity to facilitate
712 parasitism," *Sci. Rep.*, vol. 6, no. 1, Art. no. 1, Jan. 2016, doi: 10.1038/srep19443.
- 713
- 714
- 715
- 716

A



B



C



717

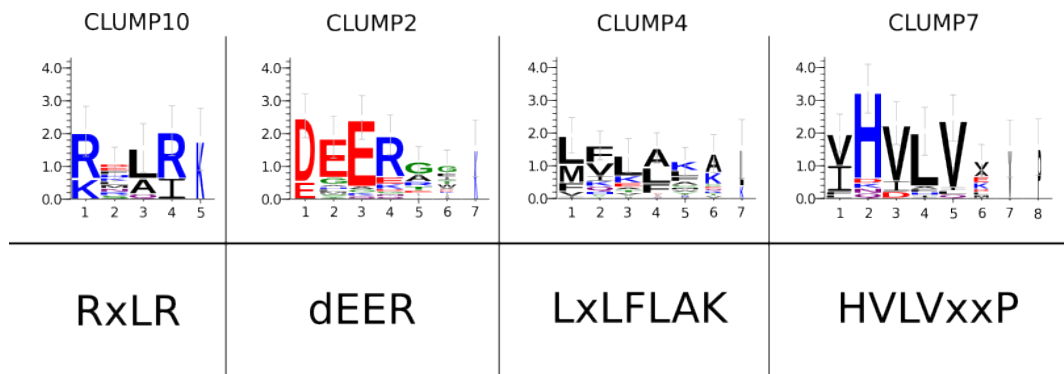
718 **Figure 1: MONSTER pipeline scheme.**

719 (A) MONSTER pipeline is composed of three steps. It takes two FASTA protein sequences datasets

720 (positive and negative) and a list of predicted motifs (enriched in the positive dataset) as input. The

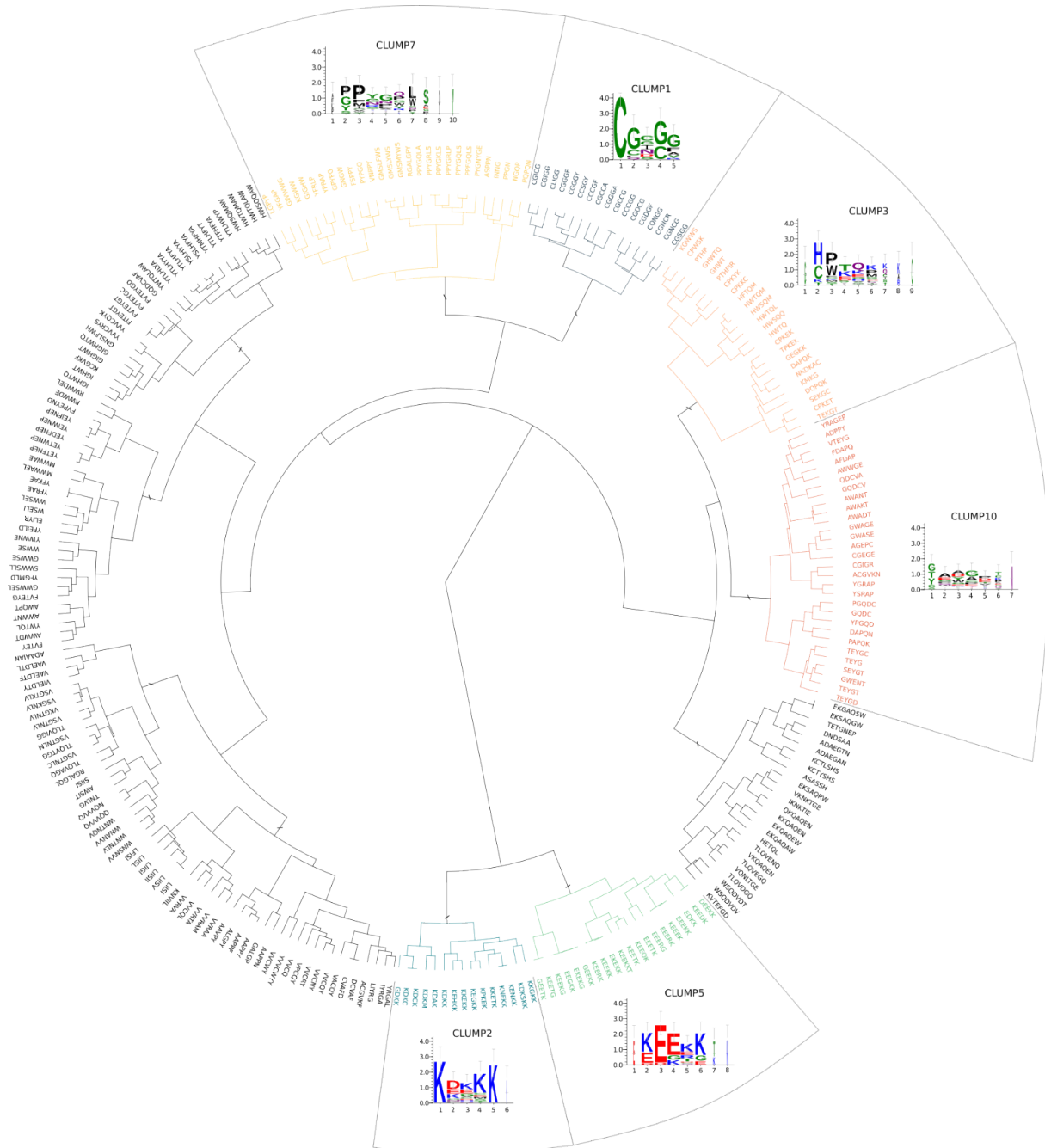
721 output is a list of CLUMPs and an associated MONSTER score. The MONSTER score is constituted

722 by: (B) CLUMP_{score} calculation. (C) Two modified Jaccard Indexes.



723 **Figure 2: Motif logos of CLUMPs compared to the target motifs.**
724 Upper-panel: alignments of motifs in the respective CLUMP are produced by PROMOCA, and then the
725 aligned motif sequences are used to produce the logos with WebLogo3. The x-axis represents the AA
726 position in the motif, while the y-axis represents log-transformed frequencies translated into bits of
727 information. Lower-panel: characteristic motifs of oomycetes effectors families from literature.
728
729
730
731

732



733

734

Figure 3: Dendrogram of CLUMPs in Plant Parasitic Nematodes (PPNs)

735

11 CLUMPs produced by MOnSTER (indicated with "P" sign). The coloured ones are those selected as

736

best-scoring CLUMPs after MOnSTER-score calculation. Each best-scoring CLUMP is associated with

737

the corresponding motif logo; alignment of motifs in each CLUMP is produced by PROMOCA and then

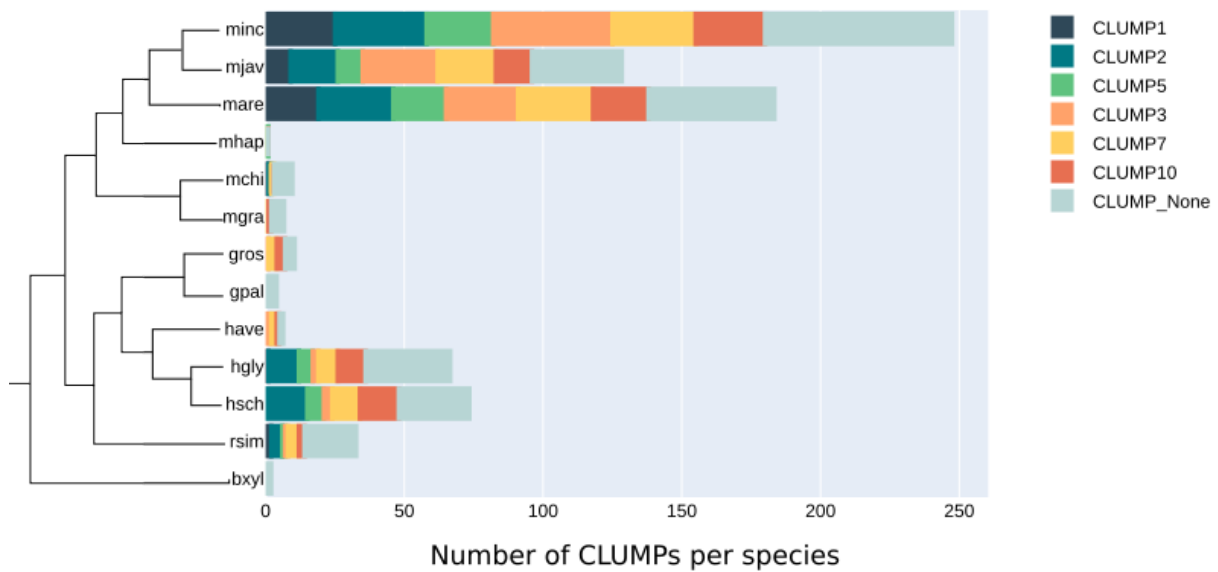
738

WebLogo 3 is used to produce the image (the x-axis shows the AA position of the motif and the y-axis

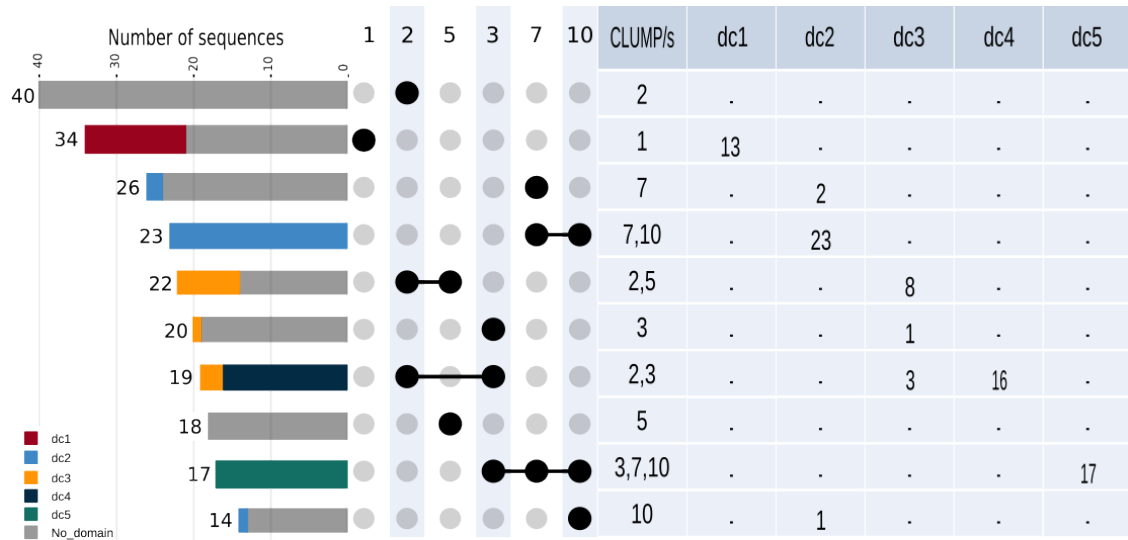
739

represents the log-transformed frequency of each AA in terms of bits of information).

740



741 **Figure 4: Cardinality of CLUMPs-motifs in each PPN species considered.**
742 The total number of motifs belonging to each significant CLUMP per PPN species accordingly to their
743 phylogeny. (minc: *Meloidogyne incognita*, mjav: *Meloidogyne javanica*, mare: *Meloidogyne arenaria*,
744 mhap: *Meloidogyne hapla*, mchi: *Meloidogyne chitwoodi*, mgra: *Meloidogyne graminicola*, gros:
745 *Globodera rostochiensis*, gpal: *Globodera pallida*, have: *Heterodera havenae*, hgly: *Heterodera*
746 *glycines*, hsch: *Heterodera schachtii*, rsim: *Radopholus similis*, bxyl: *Bursaphelenchus xylophilus*)
747



748
749
750
751
752
753
754
755
756

Figure 5: Effector proteins showing the presence of CLUMP/s associated with pathogenicity-related protein domain/s.

The table on the right shows the co-occurrence of CLUMP or CLUMPs with specific domain classes (dc); dc1, pectate lyase domain class, dc2, glycosyl hydrolase family 5 domain class, dc3 Stichodactyla toxin (ShK) domain class, dc4 14-3-3 family domain class and dc5, cysteine-rich domain class. The upset plot on the left represents the occurrences and co-occurrences of respective CLUMPs in the positive dataset, highlighting the sequences that also have an interesting protein domain following the table counts.